Crystallization and initial crystallographic characterization of the *Corynebacterium glutamicum* nitrilotriacetate monooxygenase component A

Kyung-Jin Kim,[a]* **Sujin Kim,**[b] **Sujin Lee,**[a] **Beom Sik Kang,**[c] **Heung-Soo Lee,**[a] **Tae-Kwang Oh**[b] **and Myung Hee Kim**[b]*

[a]Beamline Division, Pohang Accelerator Laboratory, Pohang, Kyungbuk 790-784, South Korea, [b]21C Frontier Microbial Genomics and Applications Center, KRIBB, Daejeon 305-806, South Korea, and [c]School of Life Science and Biotechnology, Kyungpook National University, Daegu 702-701, South Korea

Correspondence e-mail: kkj@postech.ac.kr, mhk8n@kribb.re.kr

Safety and environmental concerns have recently dictated the proper disposal of nitrilotriacetate (NTA). Biodegradation of NTA is initiated by NTA monooxygenase, which is composed of two proteins: component A and component B. The NTA monooxygenase component A protein from *Corynebacterium glutamicum* was crystallized using the sitting-drop vapour-diffusion method in the presence of ammonium sulfate as the precipitant. X-ray diffraction data were collected to a maximum resolution of 2.5 Å on a synchrotron beamline. The crystal belongs to the monoclinic space group $C2$, with unit-cell parameters $a = 111.04$, $b = 98.51$, $c = 171.61$ Å, $\beta = 101.94°$. The asymmetric unit consists of four molecules, corresponding to a packing density of 2.3 Å^3 Da^{-1}. The structure was solved by molecular replacement. Structure refinement is in progress.

1. Introduction

The synthetic chelating agent nitrilotriacetate (NTA) has been widely used for various radionuclide-processing and decontamination procedures, such as textile, paper and pulp processing and water treatment. The extensive use of NTA has led to considerable concern about the potential of NTA to remobilize radionuclides and toxic heavy metals from soils and sediments (Anderson *et al.*, 1985; Bucheli-Witschel & Egli, 2001). Such undesirable environmental consequences would cause direct health problems or affect agricultural crops and livestock, with potential transfer of toxic substances to human beings through the food chain.

A number of NTA-degrading bacterial strains have been isolated and biochemical and genetic studies on NTA degradation are being pursued (Bucheli-Witschel & Egli, 2001; Egli, 2001). NTA monooxygenase (NTA_MO) is an enzyme responsible for the oxidative cleavage of NTA to iminodiacetate (IDA) and glyoxylate. The enzyme catalyzes the hydroxylation of an α-carbon of NTA, resulting in the spontaneous formation of IDA and glyoxylate (Firestone & Tiedje, 1978; Fig. 1). NTA_MO activity requires a unique two-enzyme system composed of components A and B. Component A (NTA_MO_A) is a monooxygenase that oxidizes NTA at the expense of reduced flavin mononucleotide (FMNH$_2$) and O$_2$, whereas
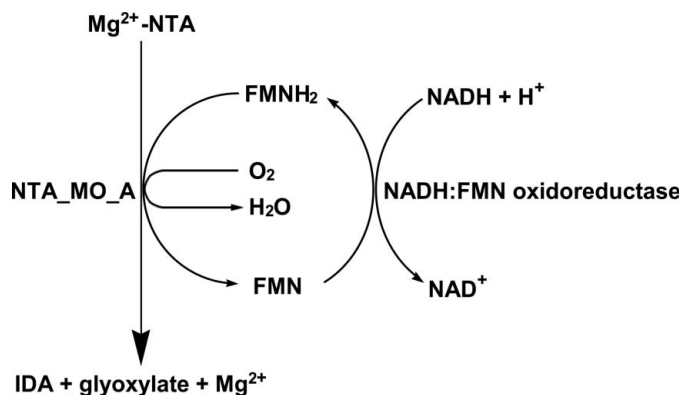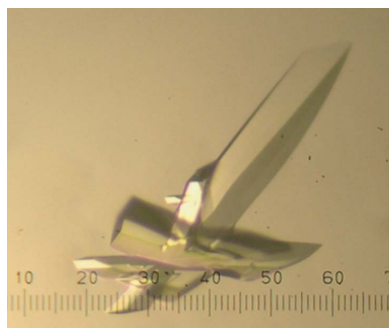
Figure 1
Proposed NTA degradation catalyzed by the two-enzyme system composed of component A (NTA_MO_A) and component B (NADH:FMN oxidoreductase).

component B is a reduced nicotinamide adenine dinucleotide (NADH):FMN oxidoreductase that provides FMNH$_2$ for NTA oxidization by using NADH to reduce FMN to FMNH$_2$. Component B can be substituted by any enzyme that can provide reduced FMN, suggesting that NTA_MO_A plays the central role in NTA_MO biodegradation of NTA (Xu *et al.*, 1997).

To date, no structure–function study has been reported for NTA_MO_A, although a crystal structure of the *Bacillus subtilis* Ytnj protein annotated as NTA_MO_A has been deposited in the Protein Data Bank (PDB) with PDB code 1yw1. However, there are no published studies on the catalytic mechanism of Ytnj. As a step towards elucidating the enzyme mechanism of NTA_MO_A, we recently cloned its gene from *Corynebacterium glutamicum* ATCC 13032, purified it and assessed its ability to oxidize NTA using FMNH$_2$ generated by an NADH:FMN oxidoreductase (Roche Applied Science) from *Photobacterium fischeri* (unpublished results). We obtained crystals of the NTA_MO_A protein. The crystals diffracted well and data were collected to a resolution of 2.5 Å. Here, we describe the crystallization and initial X-ray crystallographic analysis of the NTA_MO_A protein.

2. Expression and purification of the recombinant NTA_MO component A protein

The gene encoding NTA_MO_A was amplified from *C. glutamicum* chromosomal DNA by the polymerase chain reaction (PCR) using the following primers: 5′-GCGCGCATATGACACCGAAAGAAA-TACACCTCAAC-3′ and 5′-GCGCGCTCGAGTTAAACAAGTG-ACACCGGGCTGAATAAG-3′. The primers carried *Nde*I and *Xho*I restriction-enzyme sites at their 5′ and 3′ ends, respectively. The resulting PCR product was cloned into the pPosKJ expression vector (Kwon *et al.*, 2005), which resulted in the expression of NTA_MO_A fused to a hexahistidine tag and bacterial haemoglobin (6×His-VHb) at its N-terminus. *Escherichia coli* B834 cells transformed with the resulting plasmid, termed pPosKJ:*nta_mo_A*, were then used to produce 6×His-VHb-fused NTA_MO_A protein as follows. A 20 ml overnight culture was inoculated into 1 l of Luria–Bertani (LB) medium containing 100 µg ml^{-1} ampicillin, which was then incubated at 310 K. When the culture reached log phase (OD$_{600}$ = 0.6), expression of the 6×His-VHb-fused protein was induced by adding

isopropyl β-D-thiogalactoside to a final concentration of 1 m*M*. The cells were grown for an additional 16 h at 293 K. Harvested cells, which were red in colour, were resuspended in buffer *A* (20 m*M* Tris–HCl pH 8.0, 5 m*M* β-mercaptoethanol) and disrupted by ultra-sonication. The crude cell extracts were centrifuged at 11 000*g* for 1 h at 277 K. The target proteins from the clarified cell lysates were loaded onto an Ni–NTA column (Qiagen) equilibrated with buffer *A*. After washing the column with buffer *A* containing 20 m*M* imidazole, bound proteins were eluted with buffer *A* containing 300 m*M* imidazole. The eluted fraction was loaded onto a HiTrap Q anion-exchange column (Amersham Biosciences) and the bound proteins were eluted using a 0–500 m*M* linear gradient of NaCl. The 6×His-VHb was removed by incubation with recombinant tobacco etch virus (rTEV) protease (Invitrogen) and passage through an Ni–NTA column. After purification, NTA_MO_A still had a two-residue cloning artifact (Gly His) at its N-terminus. The final yield of the protein was approximately 50 mg per litre of cell culture. The purified protein was dialyzed against 20 m*M* Tris–HCl pH 7.0 containing 5 m*M* β-mercaptoethanol, concentrated to 20 mg ml^{-1} and stored at 193 K for use in crystallization trials. The homogeneity of the recombinant NTA_MO_A was assessed by 12% SDS–PAGE and Coomassie Brilliant Blue staining (Fig. 2).

The molecular weight of the purified protein was analyzed by size-exclusion chromatography. The purified NTA_MO_A protein was loaded onto a Superdex 75 column equilibrated with 50 m*M* Tris pH 8.0 and 150 m*M* NaCl. Size-exclusion chromatography showed the molecular weight of NTA_MO_A to be approximately 100 kDa (data not shown), whereas SDS–PAGE suggested a molecular weight of approximately 47.8 kDa (Fig. 2), indicating that NTA_MO_A probably exists as a homodimer under physiological conditions.

3. Crystallization

Crystallization of the purified protein was initially performed with commercially available sparse-matrix screens from Hampton Research and Emerald Biostructures using the sitting-drop vapour-diffusion technique at 295 K. Each experiment consisted of mixing 1 µl protein solution (20 mg ml^{-1} in 20 m*M* Tris–HCl pH 7.0 and 5 m*M* β-mercaptoethanol) with 1 µl reservoir solution and then equilibrating it against the reservoir solution. After several steps that improved the crystallization process, crystals appeared in 5–6 d and reached their maximal dimensions of approximately 300 × 50 × 50 µm using reservoir solution containing 1.6 *M* NH$_2$SO$_4$, 0.1 *M* NaCl and 0.1 *M* HEPES pH 7.5 (Fig. 3).
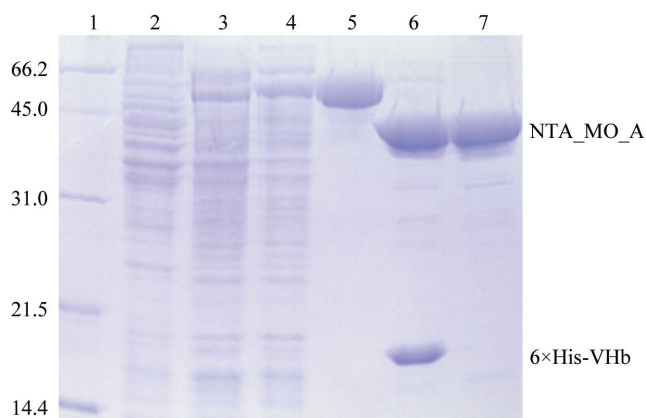

Figure 2
Expression and purification of NTA_MO_A protein as judged by SDS–PAGE. Lane 1, protein size markers (kDa); lane 2, uninduced cell lysate; lane 3, induced cell lysate; lane 4, soluble fraction; lane 5, 6×His-VHb-fused NTA_MO_A protein eluted from the Ni–NTA column; lane 6, rTEV protease-treated protein; lane 7, purified NTA_MO_A protein.
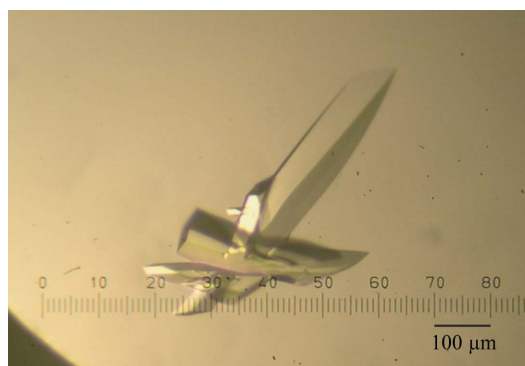

Figure 3
Monoclinic crystals of the NTA_MO_A protein from *C. glutamicum*. The crystals are ∼300 µm in the largest dimension.

Table 1
Data-collection and processing statistics.

Values in parentheses are for the highest resolution shell.

Beamline	4A (MXW), PAL
Wavelength (Å)	1.0000
Temperature (K)	100
Crystal-to-detector distance (mm)	200
Rotation range per image (°)	1.0
Total rotation range (°)	360
Space group	$C2$
Unit-cell parameters (Å, °)	$a = 111.041$, $b = 98.508$, $c = 176.606$, $\beta = 101.939$
Resolution limits (Å)	50.0–2.50 (2.59–2.50)
Total reflections	241884
Unique reflections	62001
Completeness (%)	96.7 (84.6)
R_{merge}† (%)	10.1 (43.8)
$\langle I/\sigma(I)\rangle$	11.1 (2.3)

† $R_{merge} = \sum_{hkl}\sum_i |I_i - I_m|/\sum_{hkl}\sum_i I_i$, where I_i and I_m are the observed individual and mean intensities of a reflection, respectively. $\sum_i$ is the sum over the individual measurements of a reflection and $\sum_{hkl}$ is the sum over all reflections.

4. X-ray analysis

The crystals were transferred to cryoprotectant solution containing 1.7 M NH$_2$SO$_4$, 0.1 M NaCl, 0.1 M HEPES pH 7.5 and 25%(v/v) glycerol, fished out with a loop larger than the crystals and flash-frozen by immersion in liquid nitrogen at 100 K. The data were collected to a resolution of 2.5 Å at beamline 4A (MXW), which incorporated a Quantum 210 CCD detector (ADSC, USA), at the Pohang Accelerator Laboratory (PAL, Pohang, Korea). A total of 360 images were collected with an oscillation angle of 1° and an exposure time of 5 s per image. The data were indexed, integrated, and scaled using the *HKL*-2000 package (Otwinowski & Minor, 1997). The NTA_MO_A crystals belong to the centred monoclinic space group $C2$, with unit-cell parameters $a = 111.04$, $b = 98.51$, $c = 171.61$ Å, $\beta = 101.94°$. Assuming four molecules of NTA_MO_A per asymmetric unit, the crystal volume per unit of protein weight was 2.3 Å^3 Da^{-1} (Matthews, 1968), which corresponds to a solvent content of approximately 46.5%. Crystallographic data statistics are summarized in Table 1.

The structure of NTA_MO_A appears to have been solved by molecular replacement. The *B. subtilis* Ytnj protein (PDB code 1yw1) with side chains converted to Ala was used as the search model. The identity and similarity of the 1yw1 sequence to NTA_MO_A are 37 and 57%, respectively. *MOLREP* (Vagin & Teplyakov, 1997) located four poly-Ala model molecules in the asymmetric unit, forming two dimers. The resulting solution had a correlation coefficient and R factor of 0.426 and 62.1%, respectively. After rigid-body refinement using *REFMAC*5 (Murshudov *et al.*, 1997) from the *CCP*4 suite in the resolution range 40–2.5 Å, R and R_{free} were 45.6 and 54.0%, respectively, with a correlation coefficient of 0.671. The initial electron-density map, which was of good quality with backbones well defined by electron density, allowed us to build a three-dimensional NTA_MO_A model. Crystallographic model building and refinement of the structure to 2.5 Å resolution is in progress.

References

Anderson, R. L., Bishop, W. E. & Campbell, R. L. (1985). *Crit. Rev. Toxicol.* **15**, 1–102.
Bucheli-Witschel, M. & Egli, T. (2001). *FEMS Microbiol. Rev.* **25**, 69–106.
Egli, T. (2001). *J. Biosci. Bioeng.* **92**, 89–97.
Firestone, M. K. & Tiedje, J. M. (1978). *Appl. Environ. Microbiol.* **35**, 955–961.
Kwon, S. Y., Choi, Y. J., Kang, T. H., Lee, K. H., Cha, S. S., Kim, G. H., Lee, H. S., Kim, K. T. & Kim, K. J. (2005). *Plasmids*, **53**, 274–282.
Matthews, B. W. (1968). *J. Mol. Biol.* **33**, 491–497.
Murshudov, G. N., Vagin, A. A. & Dodson, E. J. (1997). *Acta Cryst.* D**53**, 240–255.
Otwinowski, Z. & Minor, W. (1997). *Methods Enzymol.* **276**, 307–326.
Vagin, A. & Teplyakov, A. (1997). *J. Appl. Cryst.* **30**, 1022–1025.
Xu, Y., Mortimer, M. W., Fisher, T. S., Kahn, M. L. & Brockman, F. J. (1997). *J. Bacteriol.* **179**, 1112–1116.